NASA Tech Briefs

NATIONAL AERONAUTICS AND SPACE ADMINISTRATION

⊕ **Technology Focus**

〰 **Electronics/Computers**

◉ **Software**

⬡ **Materials**

⊗ **Mechanics**

✿ **Machinery/Automation**

⊒ **Manufacturing & Prototyping**

⬗ **Bio-Medical**

⊛ **Physical Sciences**

⊘ **Information Sciences**

⧉ **Books and Reports**

INTRODUCTION

Tech Briefs are short announcements of innovations originating from research and development activities of the National Aeronautics and Space Administration. They emphasize information considered likely to be transferable across industrial, regional, or disciplinary lines and are issued to encourage commercial application.

Availability of NASA Tech Briefs and TSPs

Requests for individual Tech Briefs or for Technical Support Packages (TSPs) announced herein should be addressed to

National Technology Transfer Center

Telephone No. **(800) 678-6882** or via World Wide Web at **www2.nttc.edu/leads/**

Please reference the control numbers appearing at the end of each Tech Brief. Information on NASA's Innovative Partnerships Program (IPP), its documents, and services is also available at the same facility or on the World Wide Web at **http://ipp.nasa.gov**.

Innovative Partnerships Offices are located at NASA field centers to provide technology-transfer access to industrial users. Inquiries can be made by contacting NASA field centers listed below.

NASA Field Centers and Program Offices

Ames Research Center
Lisa L. Lockyer
(650) 604-1754
lisa.l.lockyer@nasa.gov

Dryden Flight Research Center
Gregory Poteat
(661) 276-3872
greg.poteat@dfrc.nasa.gov

Goddard Space Flight Center
Nona Cheeks
(301) 286-5810
nona.k.cheeks@nasa.gov

Jet Propulsion Laboratory
Ken Wolfenbarger
(818) 354-3821
james.k.wolfenbarger@jpl.nasa.gov

Johnson Space Center
Michele Brekke
(281) 483-4614
michele.a.brekke@nasa.gov

Kennedy Space Center
David R. Makufka
(321) 867-6227
david.r.makufka@nasa.gov

Langley Research Center
Martin Waszak
(757) 864-4015
martin.r.waszak@nasa.gov

Glenn Research Center
Robert Lawrence
(216) 433-2921
robert.f.lawrence@nasa.gov

Marshall Space Flight Center
Vernotto McMillan
(256) 544-2615
vernotto.mcmillan@msfc.nasa.gov

Stennis Space Center
John Bailey
(228) 688-1660
john.w.bailey@nasa.gov

Carl Ray, Program Executive
Small Business Innovation Research (SBIR) & Small Business Technology Transfer (STTR) Programs
(202) 358-4652
carl.g.ray@nasa.gov

Merle McKenzie, Director
Innovative Partnerships Program Office
(202) 358-2560
merle.mckenzie-1@nasa.gov

Tech Briefs

NATIONAL AERONAUTICS AND SPACE ADMINISTRATION

Calibration Test Set for a Phase-Comparison Digital Tracker

Four equal-amplitude signals are generated at selectable phase increments of 0.1°.

NASA's Jet Propulsion Laboratory, Pasadena, California

An apparatus that generates four signals at a frequency of 7.1 GHz having precisely controlled relative phases and equal amplitudes has been designed and built. This apparatus is intended mainly for use in computer-controlled automated calibration and testing of a phase-comparison digital tracker (PCDT) that measures the relative phases of replicas of the same X-band signal received by four antenna elements i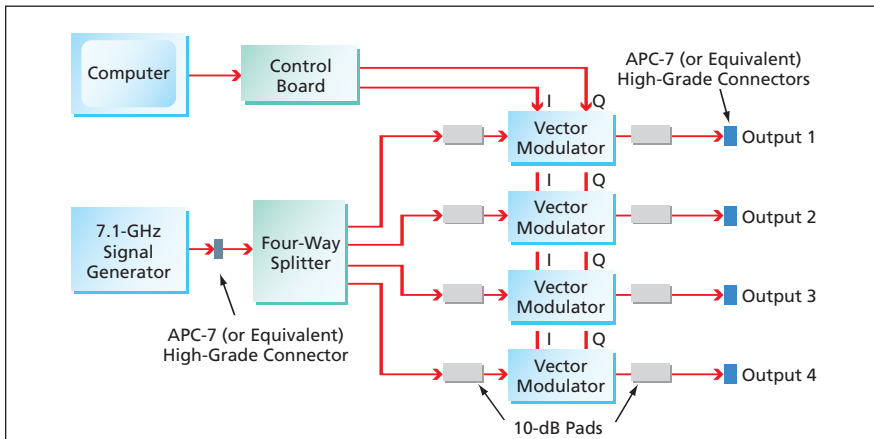n an array. (The relative direction of incidence of the signal on the array is then computed from the relative phases.) The present apparatus can also be used to generate precisely phased signals for steering a beam transmitted from a phased antenna array.

The apparatus (see figure) includes a 7.1-GHz signal generator, the output of which is fed to a four-way splitter. Each of the four splitter outputs is attenuated by 10 dB and fed as input to a vector modulator, wherein DC bias voltages are used to control the in-phase (I) and quadrature (Q) signal components. The bias voltages are generated by digital-to-analog-converter circuits on a control board that receives its digital control input from a computer running a LabVIEW program. The outputs of the vector modulators are further attenuated by 10 dB, then presented at high-grade radio-frequency connectors. The attenuation reduces the effects of changing mismatch and reflections.

The apparatus was calibrated in a process in which the bias voltages were first stepped through all possible IQ settings. Then in a reverse interpolation performed by use of MATLAB software, a lookup table containing 3,600 IQ settings, representing equal amplitude and phase increments of 0.1°, was created for each vector modulator. During operation of the apparatus, these lookup tables are used in calibrating the PCDT.

This work was done by Amy Boas, Samuel Li, and Robert McMaster of Caltech for **NASA's Jet Propulsion Laboratory.** *Further information is contained in a TSP (see page 1).*
NPO-42813

The **PCDT Calibration Test Set** contains four computer-controlled vector modulators that produced selectably phased replicas of a 7.1-GHz input signal.

Wireless Acoustic Measurement System

This system supplants older, less-capable, cable-connected systems.

Stennis Space Center, Mississippi

A prototype wireless acoustic measurement system (WAMS) is one of two main subsystems of the Acoustic Prediction/ Measurement Tool, which comprises software, acoustic instrumentation, and electronic hardware combined to afford integrated capabilities for predicting and measuring noise emitted by rocket and jet engines. The other main subsystem is described in the article on page 8.

The WAMS includes analog acoustic measurement instrumentation and analog and digital electronic circuitry combined with computer wireless local-area networking to enable (1) measurement of sound-pressure levels at multiple locations in the sound field of an engine under test and (2) recording and processing of the measurement data. At each field location, the measurements are taken by a portable unit, denoted a field station. There are ten field stations, each of which can take two channels of measurements.

Each field station is equipped with two instrumentation microphones, a micro-ATX computer, a wireless network adapter, an environmental enclosure, a directional radio antenna, and a battery power supply. The environmental enclosure shields the computer from weather and from extreme acoustically induced vibrations. The power supply is based on a marine-service lead-acid storage battery that has enough capacity to support operation for as long as 10 hours.

A desktop computer serves as a control server for the WAMS. The server is connected to a wireless router for communication with the field stations via a wireless local-area network that complies with wireless-network standard 802.11b of the Institute of Electrical and Electronics Engineers. The router and the

wireless network adapters are controlled by use of Linux-compatible driver software. The server runs custom Linux software for synchronizing the recording of measurement data in the field stations. The software includes a module that provides an intuitive graphical user interface through which an operator at the control server can control the operations of the field stations for calibration and for recording of measurement data.

A test engineer positions and activates the WAMS. The WAMS automatically establishes the wireless network. Next, the engineer performs pretest calibrations. Then the engineer executes the test and measurement procedures. After the test, the raw measurement files are copied and transferred, through the wireless network, to a hard disk in the control server. Subsequently, the data are processed into ⅓-octave spectrograms.

✿ Spiral Orbit Tribometer
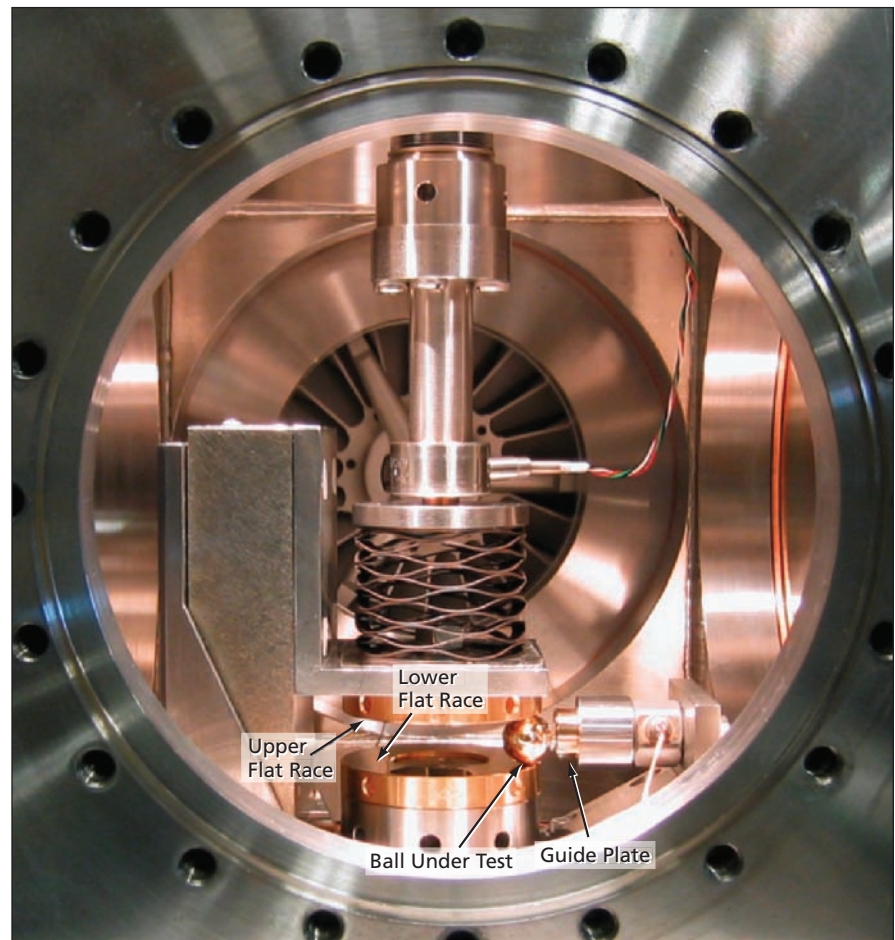### Friction and lubricant degradation rate can be quantified rapidly.

John H. Glenn Research Center, Cleveland, Ohio

The spiral orbit tribometer (SOT) bridges the gap between full-scale life testing and typically unrealistic accelerated life testing of ball-bearing lubricants in conjunction with bearing ball and race materials. The SOT operates under realistic conditions and quickly produces results, thereby providing information that can guide the selection of lubricant, ball, and race materials early in a design process.

The SOT is based upon a simplified, retainerless thrust bearing comprising one ball between flat races (see figure). The SOT measures lubricant consumption and degradation rates and friction coefficients in boundary lubricated rolling and pivoting contacts.

The ball is pressed between the lower and upper races with a controlled force and the lower plate is rotated. The combination of load and rotation causes the ball to move in a nearly circular orbit that is, more precisely, an opening spiral. The spiral's pitch is directly related to the friction coefficient. At the end of the orbit, the ball contacts the guide plate, restoring the orbit to its original radius. The orbit is repeatable throughout the entire test. A force transducer, mounted in-line with the guide plate, measures the force between the ball and the guide plate, which directly relates to the friction coefficient. The SOT, shown in the figure, can operate in under ultra-high vacuum (10^{-9} Torr) or in a variety of gases at atmospheric pressure. The load force can be adjusted between 45 and 450 N. By varying the load force and ball diameter, mean Hertzian stresses between 0.5 and 5.0 GPa can be obtained. The ball's orbital speed range is between 1 and 100 rpm.

The **Spiral-Orbit Tribometer** is based on a retainerless flat thrust bearing. The ball is squeezed between the upper and lower flat races while the lower flat race is rotated, causing the ball to orbit in an opening spiral.

For most of the orbit, the ball undergoes pure rolling with pivot; however, when the ball contacts the guide plate, sliding also occurs. The period of contact with the guide plate, termed the "scrub," is the most tribologically severe part of the orbit and is when the majority of the lubricant's tribo-degradation occurs.

Typically, a small amount of lubricant (≈50 µg) is applied to the ball at the beginning of a test. Such a minute lubricant amount usually degrades within one or two days. The test duration can be varied by adjusting the initial amount of lubricant and/or the load force. A test is terminated when the lu-

bricant fails. Failure is defined when the friction coefficient rises beyond a predefined limit, which is usually two to three times the starting friction coefficient. The lifetime of the lubricant is then quantified as the total number of ball orbits completed divided by initial amount of lubricant on the ball. Typically, four tests are done for each condition and their results averaged for statistical significance in the test data. Relative lifetimes for various materials can be compared and can be directly correlated with relative lifetimes in real applications.

This work was done by Stephen V. Pepper and William R. Jones, Jr. of **Glenn Research Center***, Edward Kingsbury of Interesting Rolling Contact, and Mark J. Jansen of the University of Toledo. Further information is contained in a TSP (see page 1).*

*Inquiries concerning rights for the commercial use of this invention should be addressed to NASA Glenn Research Center, Innovative Partnerships Office, Attn: Steve Fedor, Mail Stop 4–8, 21000 Brookpark Road, Cleveland, Ohio 44135. Refer to LEW-17912-**1**.*

Arrays of Miniature Microphones for Aeroacoustic Testing
MEMS microphones are mounted on flexible printed-circuit boards.

Langley Research Center, Hampton, Virginia

A phased-array system comprised of custom-made and commercially available microelectromechanical system (MEMS) silicon microphones and custom ancillary hardware has been developed for use in aeroacoustic testing in hard-walled and acoustically treated wind tunnels. Recent advances in the areas of multi-channel signal processing and beam forming have driven the construction of phased arrays containing ever-greater numbers of microphones. Traditional obstacles to this trend have been posed by (1) the high costs of conventional condenser microphones, associated cabling, and support electronics and (2) the difficulty of mounting conventional microphones in the precise locations required for high-density arrays. The present development overcomes these obstacles.

One of the hallmarks of the new system is a series of fabricated platforms on which multiple microphones can be mounted. These mounting platforms, consisting of flexible polyimide circuit-board material (see left side of figure), include all the necessary microphone power and signal interconnects. A single bus line connects all microphones to a common power supply, while the signal lines terminate in one or more data buses on the sides of the circuit board. To minimize cross talk between array channels, ground lines are interposed as shields between all the data bus signal lines. The MEMS microphones are electrically connected to the boards via solder pads that are built into the printed wiring. These flexible circuit boards share many characteristics with their traditional rigid counterparts, but can be manufactured much thinner, as small as 0.1 millimeter, and much lighter with boards weighing as much as 75 percent less than traditional rigid ones.

An **Array of MEMS Microphones** (left) and a **Face Sheet** (right) are shown. The array is formed on a flexible printed-circuit board. The array can readily be affixed to a curved wind-tunnel surface for use in aeroacoustic testing. The face sheet containing small rectangular cutouts for the microphones is placed over an array like that on the left to provide a smooth outer surface.

For a typical hard-walled wind-tunnel installation, the flexible printed-circuit board is bonded to the tunnel wall and covered with a face sheet that contains precise cutouts for the microphones. Once the face sheet is mounted, a smooth surface is established over the entire array due to the flush mounting of all microphones (see right side of figure). The face sheet is made from a continuous glass-woven-fabric base impregnated with an epoxy resin binder. This material offers a combination of high mechanical strength and low dielectric loss, making it suitable for withstanding the harsh test section environment present in many wind tunnels, while at the same time protecting the underlying polyimide board.

Customized signal-conditioning hardware consisting of line drivers and anti-aliasing filters are coupled with the array. The line drivers are constructed using low-supply-current, high-gain-bandwidth operational amplifiers designed to transmit the microphone signals several dozen feet from the array to external acquisition hardware. The anti-alias filters consist of individual Chebyshev low-pass filters (one for each microphone channel) housed on small printed-circuit boards mounted on one or more motherboards. The mother/daughter board design results in a modular system, which is easy to debug and service and which enables the filter characteristics to be changed by swapping daughter boards with ones containing different filter parameters. The filter outputs are passed to commercially-available acquisition hardware to digitize and store the conditioned microphone signals. Wind-tunnel testing of the new MEMS microphone polyimide mounting system shows that the array performance is comparable to that of traditional arrays, but with significantly less cost of construction.

This work was done by Qamar A. Shams, William M. Humphreys, Bradley S. Sealey, Scott M. Bartram, Allan J. Zuckerwar, Toby Comeaux, and James K. Adams of **Langley Research Center***. Further information is contained in a TSP (see page 1). LAR-17171-1*

Predicting Rocket or Jet Noise in Real Time

Measurement data can be analyzed in real time.

Stennis Space Center, Mississippi

A semi-empirical theoretical model and a C++ computer program that implements the model have been developed for use in predicting the noise generated by a rocket or jet engine. The computer program, entitled the Realtime Rocket and Jet Engine Noise Analysis and Prediction Software, is one of two main subsystems of the Acoustic Prediction/Measurement Tool, which comprises software, acoustic instrumentation, and electronic hardware combined to afford integrated capabilities for real-time prediction and measurement of noise emitted by rocket and jet engines. [The other main subsystem, consisting largely of acoustic instrumentation and electronic hardware, is described in "Wireless Acoustic Measurement System," which appears elsewhere in this section.]

The theoretical model was derived from the fundamental laws of fluid mechanics, as first was done by M. J. Lighthill in his now famous theory of aerodynamically generated sound. The far-field approximation of the Lighthill theory is incorporated into this model. Many other contributions from various researchers have also been introduced into the model. The model accounts for two noise components: shear noise and self noise. The final result of the model is expressed in terms of a volume integral of the acoustic intensities attributable to these two components, subject to various directivity coefficients.

The computer program was written to solve the volume integral. The inputs required by the program are two data files from a computational fluid dynamics (CFD) simulation of the flow of interest: the computational-grid file and the solution file. The CFD solution should be one that has been obtained for conditions that closely approximate those of an experimental test that is yet to be performed.

In the current state of development of the model and software, it is recommended that the observation points lie along a radius at an angle >60° from the jet axis. The software provides, and is driven via, a graphical user interface, which facilitates its use. Optionally, the program accepts additional input in the form of data on the measured sound pressure level as a function of frequency at a given far-field location, preferably at an angle of 90° from the jet axis. The user is prompted to use default empirical constants or to choose constants based the measurement data. The user can view the results and compare them with other computational or experimental data. Once satisfied with the results, the user can save a graph of the results in a file that can be imported into documents.

This program was written by Kader Frendi of the University of Alabama in Huntsville for **Stennis Space Center**.

In accordance with Public Law 96-517, the contractor has elected to retain title to this invention. Inquiries concerning rights for its commercial use should be addressed to:

Dr. Kader Frendi
The University of Alabama
5000 Technology Drive, Room THN264
Huntsville, AL 35899
Phone No.: (256) 824-7206
E-mail: frendi@eng.uah.edu
Refer to SSC-00215-1, volume and number of this NASA Tech Briefs *issue, and the page number.*

Computational Workbench for Multibody Dynamics

NASA's Jet Propulsion Laboratory, Pasadena, California

PyCraft is a computer program that provides an interactive, workbenchlike computing environment for developing and testing algorithms for multibody dynamics. Examples of multibody dynamic systems amenable to analysis with the help of PyCraft include land vehicles, spacecraft, robots, and molecular models. PyCraft is based on the Spatial-Operator-Algebra (SOA) formulation for multibody dynamics. The SOA operators enable construction of simple and compact representations of complex multibody dynamical equations. Within the PyCraft computational workbench, users can, essentially, use the high-level SOA operator notation to represent the variety of dynamical quantities and algorithms and to perform computations interactively. PyCraft provides a Python-language interface to underlying C++ code. Working with SOA concepts, a user can create and manipulate Python-level operator classes in order to implement and evaluate new dynamical quantities and algorithms. During use of PyCraft, virtually all SOA-based algorithms are available for computational experiments.

This program was written by Abhinandan Jain of Caltech for **NASA's Jet Propulsion Laboratory**. *Further information is contained in a TSP (see page 1).*

This software is available for commercial licensing. Please contact Karina Edmonds of the California Institute of Technology at (626) 395-2322. Refer to NPO-42891.

High-Power, High-Efficiency Ka-Band Space Traveling-Wave Tube

Improved designs of critical components contribute to increased power and efficiency.

John H. Glenn Research Center, Cleveland, Ohio

The L-3 Communications Model 999H traveling-wave tube (TWT) has been demonstrated to generate an output power of 144 W at 60-percent overall efficiency in continuous-wave operation over the frequency band from 31.8 to 32.3 GHz. The best TWT heretofore commercially available for operation in the affected frequency band is characterized by an output power of only 35 W and an efficiency of 50 percent. Moreover, whereas prior TWTs are limited to single output power levels, it has been shown that the output power of the Model 999H can be varied from 54 to 144 W.

A TWT is a vacuum electronic device used to amplify microwave signals. TWTs are typically used in free-space communication systems because they are capable of operating at power and efficiency levels significantly higher than those of solid-state devices. In a TWT, an electron beam is generated by an electron gun consisting of a cathode, focusing electrodes, and an anode. The electrons pass through a hole in the anode and are focused into a cylindrical beam by a stack of periodic permanent magnets and travel along the axis of an electrically conductive helix, along which propagates an electromagnetic wave that has been launched by an input signal that is to be amplified.

The beam travels within the helix at a velocity close to the phase velocity of the electromagnetic wave. The electromagnetic field decelerates some of the electrons and accelerates others, causing the beam to become formed into electron bunches, which further interact with the electromagnetic wave in such a manner as to surrender kinetic energy to the wave, thereby amplifying the wave. The net result is to amplify the input signal by a factor of about 100,000. After the electrons have passed along the helix, they impinge on electrodes in a collector. The collector decelerates the electrons in such a manner as to recover most of the remaining kinetic energy and thereby significantly increase the power efficiency of the TWT.

The increase in power and efficiency of L-3 Communications Model 999H TWT over those of prior TWTs are attributable to several factors:
• Beam-focusing components feature new designs for improved thermal capability and increased operating stability.
• Advanced computational modeling of the interaction of the microwave signal with the electron beam made it possible to modify designs of components to attain high efficiency over a wide range of power levels.
• Improved wide-band waveguide-to-circuit coupling and wide-band, high-power radio-frequency windows were developed.
• A four-stage depressed collector was optimized by use of MICHELLE, a Naval Research Laboratory computer code for modeling guns and collectors in TWTs.
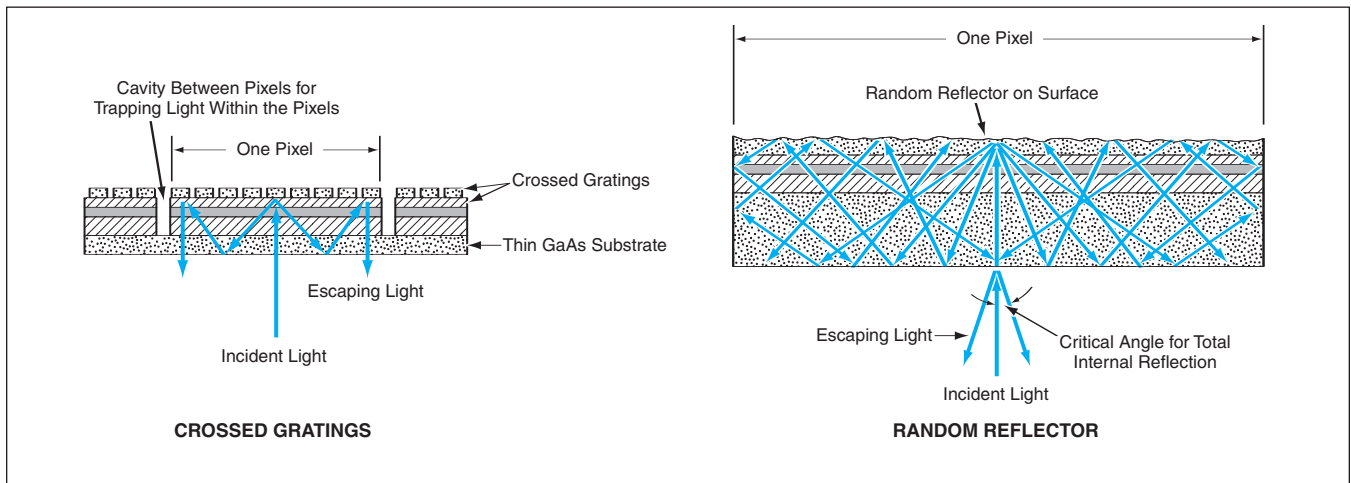
Gratings and Random Reflectors for Near-Infrared PIN Diodes

Quantum efficiency would be increased.

NASA's Jet Propulsion Laboratory, Pasadena, California

Crossed diffraction gratings and random reflectors have been proposed as means to increase the quantum efficiencies of InGaAs/InP positive/intrinsic/negative (PIN) diodes designed to operate as near-infrared photodetectors. The proposal is meant especially to apply to focal-plane imaging arrays of such photodetectors to be used for near-infrared imaging. A further increase in quantum efficiency near the short-wavelength limit of the near-infrared spectrum of such a photodetector array could be effected by removing the InP substrate of the array.

The use of crossed diffraction gratings and random reflectors as optical devices for increasing the quantum efficiencies of quantum-well infrared photodetectors (QWIPs) was discussed in several prior *NASA Tech Briefs* articles. While the optical effects of crossed gratings and random reflectors as applied to PIN photodiodes would be similar to those of crossed gratings and random reflectors as applied to QWIPs, the physical mechanisms by which these optical effects would enhance efficiency differ between the PIN-photodiode and QWIP cases:
• In a QWIP, the multiple-quantum-well layers are typically oriented parallel to the focal plane and therefore perpendicular or nearly perpendicular to the direction of incidence of infrared light. By virtue of the applicable quantum selection rules, light polarized parallel to the focal plane (as normally incident light is) cannot excite charge carriers and, hence, cannot be detected. A pair of crossed gratings or a random reflector scatters normally or nearly normally incident light so that a significant portion of it attains a component of polarization normal to

Crossed Diffraction Gratings or a Random Reflector would be fabricated on the back (here, the top) face of a PIN photodiode in each pixel of an imaging array of such photodiodes.

the focal plane and, hence, can excite charge carriers.

- A pair of crossed gratings or a random reflector on a PIN photodiode would also scatter light into directions away from the perpendicular to the focal plane. However, in this case, the reason for redirecting light away from the perpendicular is to increase the length of the optical path through the detector to increase the probability of absorption of photons and thereby increase the resulting excitation of charge carriers.

A pair of crossed gratings or a random reflector according to the proposal would be fabricated as an integral part of photodetector structure on the face opposite the focal plane (see figure). In the presence of crossed gratings, light would make four passes through the device before departing. In the presence of a random reflector, a significant portion of the light would make more than four passes: After each bounce, light would be scattered at a different random angle, and would have a chance to escape only when it was reflected, relative to the normal, at an angle less than the critical angle for total internal reflection. Given the indices of refraction of the photodiode materials, this angle would be about 17°. This amounts to a very narrow cone for escape of trapped light.

Optically Transparent Split-Ring Antennas for 1 to 10 GHz

Advantages include ultra-wide-band operation, miniaturization, and excellent impedance matching.

John H. Glenn Research Center, Cleveland, Ohio

Split-ring antennas made from optically transparent, electrically conductive films have been invented for applications in which there are requirements for compact antennas capable of operation over much or all of the frequency band from 1 to 10 GHz. Primary examples of such applications include wireless local-area networks and industrial, scientific, and medical (ISM) applications. These antennas can be conveniently located on such surfaces as those of automobile windows and display screens of diverse hand-held electronic units. They are fabricated by conventional printed-circuit techniques and can easily be integrated with solid-state amplifier circuits to enhance gain.

The structure of an antenna of this type includes an antenna/feed layer supported on the top or outer face of a dielectric (e.g., glass) and, optionally, a ground layer on the bottom or inner face of the substrate. The ring can be in the form of either a conductive strip or a slot in the antenna/feed layer. The ring can be of rectangular, square, circular, elliptical, or other suitable shape and can be excited by means of a microstrip, slot line, or coplanar waveguide. For example, the antenna shown in the figure features a square conductive-strip split ring with a microstrip feed.

In general, an antenna fed at its external boundary in the manner of this invention presents very high impedance, thereby creating an impedance-matching problem. Splitting the ring — that is, cutting a notch through the ring — offers a solution to the problem in that the notch fixes the location of maximum electric field, which location is directly related to the impedance. Thus, an excellent impedance match can be achieved through proper choice of the location of the notch.

In geometric layout, such a ring antenna structure is typically between $\frac{1}{4}$ and $\frac{1}{3}$ the size of a patch antenna capable of operating in the same frequency range. This miniaturization of the antenna is desirable, not only because it contributes to overall miniaturization of equipment, but

This **Square Split-Ring Antenna** operates with a voltage standing-wave ratio of 2 or less over the entire ISM frequency band.

also because minimization of the extent of the optically transparent, electrically conductive film helps to minimize the electrical loss associated with the surface resistance (≈5 ohms per square) of the transparent, electrically conductive film material.

Incidentally, even at ≈5 ohms per square, this surface resistance is significantly less than that of indium tin oxide film (typically > 25 ohms per square), which, heretofore has been the transparent, electrically conductive film material of choice. At the time of writing this article,

information on the composition of the lower-resistance film used in the antennas of this invention was not available.

This work was done by Richard Q. Lee and Rainee N. Simons of **Glenn Research Center**. *Further information is contained in a TSP (see page 1).*

Inquiries concerning rights for the commercial use of this invention should be addressed to NASA Glenn Research Center, Innovative Partnerships Office, Attn: Steve Fedor, Mail Stop 4–8, 21000 Brookpark Road, Cleveland, Ohio 44135. Refer to LEW-17925-1.

Ice-Penetrating Robot for Scientific Exploration

A compact probe contains advanced power, instrumentation, navigation, control, and communication systems.

NASA's Jet Propulsion Laboratory, Pasadena, California

The cryo-hydro integrated robotic penetrator system (CHIRPS) is a partially developed instrumentation system that includes a probe designed to deeply penetrate the Europan ice sheet in a search for signs of life. The CHIRPS could also be used on Earth for similar exploration of the polar ice caps — especially at Lake Vostok in Antarctica. The CHIRPS probe advances downward by a combination of simple melting of ice (typically for upper, non-compacted layers of an ice sheet) or by a combination of melting of ice and pumping of meltwater (typically, for deeper, compacted layers). The heat and electric power for melting, pumping, and operating all of the onboard instrumentation and electronic circuitry are supplied by radioisotope power sources (RPSs) and thermoelectric converters energized by the RPSs. The instrumentation and electronic circuitry includes miniature guidance and control sensors and an advanced autonomous control system that has fault-management capabilities.

The CHIRPS probe is about 1 m long and 15 cm in diameter. The RPSs generate a total thermal power of 1.8 kW. Initially, as this power melts the surrounding ice, a meltwater jacket about 1 mm thick forms around the probe. The center of gravity of the probe is well forward (down), so that the probe is vertically stabilized like a pendulum. Heat is circulated to the nose by means of miniature pumps and heat pipes.

The probe melts ice to advance in a step-wise manner: Heat is applied to the nose to open up a melt void, then heat is applied to the side to allow the probe to slip down into the melt void. The melt void behind the probe is allowed to re-freeze. Four quadrant heaters on the nose and another four quadrant heaters on the rear (upper) surface of the probe are individually controllable for steering: Turning on two adjacent nose heaters on the nose and two adjacent heaters on the opposite side at the rear causes melt voids to form on opposing sides, such that the probe descends at an angle from vertical. This steering capability can be used to avoid debris trapped in the ice or to maneuver closer to a trapped object of scientific interest.

The probe contains a system that ingests meltwater, heats the water, and pumps the heated water to form a jet out of a central orifice on the nose. The jet removes debris and contributes to the melting of ice in front of the probe. The external pressure of the ice is utilized to drive some of the meltwater into a channel on the outside of the probe shell, across a membrane, into miniature pumps, which supply water samples to the onboard scientific instruments.

The guidance and control sensors include a three-axis inclinometer, a forward-looking acoustic imager, and sensors for measuring temperature, pressure, flow rate, and pump-motor current. There is also a tether-payout encoder and a tether-actuator/brake current sensor for use in the event that the probe is connected to surface instrumentation via a tether cable (typically, for a shallow penetration). The electronic circuitry includes a power conditioner, telemetry driver, master controller, digital-to-analog and analog-to-digital converters, instrument drivers, and memory circuits, including data buffers.

At the rear (upper end) of the fully developed probe, for radio communication with the surface instrumentation in the event that a tether cable was not used (typically, during a deep penetration), there would be a primary radio transceiver and its antenna. Behind this antenna there would be 13 radio relay units, denoted ice transceivers, each between 2 and 3 cm thick and about 10 cm in diameter. The transceivers would be released, one at a time, into the rear slush and allowed to become frozen in place for relaying signals between the probe and the surface. The release depths would be chosen on the basis of signal strength and of the temperature and electrical conductivity of the ice.

In the event of an ice sheet over a body of liquid water (as in Lake Vostok), as the probe approached the ice/liquid interface, the acoustic imager would sense the interface. At this point, the front portion of the probe carrying the heat source and instruments would separate from the rear portion of the probe. The ice would refreeze around the aft body, which would thereafter serve as an anchor and a communication relay. The front portion would descend through the water on a tether, sampling the water for signs of life.

This work was done by Wayne Zimmerman, Frank Carsey, and Lloyd French of Caltech for **NASA's Jet Propulsion Laboratory**. *Further information is contained in a TSP (see page 1).*
NPO-40747

Power-Amplifier Module for 145 to 165 GHz

This module represents the highest frequency solid-state power amplifier to date.

NASA's Jet Propulsion Laboratory, Pasadena, California

A power-amplifier module that operates in the frequency range of 145 to 165 GHz has been designed and constructed as a combination of (1) a previously developed monolithic microwave integrated circuit (MMIC) power amplifier and (2) a waveguide module. The amplifier chip was needed for driving a high-electron-mobility-transistor (HEMT) frequency doubler. While it was feasible to connect the amplifier and frequency-doubler chips by use of wire bonds, it was found to be much more convenient to test the amplifier and doubler chips separately. To facilitate separate testing, it was
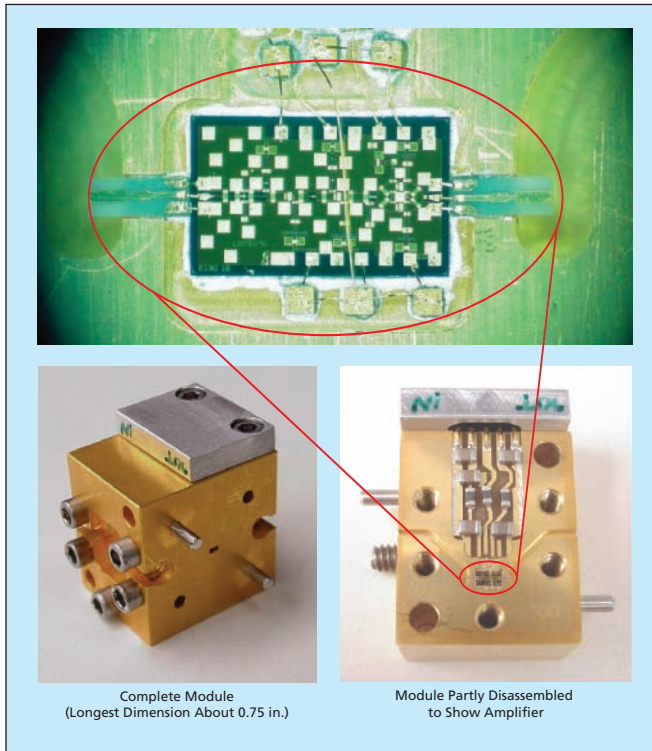

Figure 2. **Output Power and Gain** at 150 GHz were measured as functions of input power. The output power exhibited saturation at 13 dBm.

decided to package the amplifier and doubler chips in separate waveguide modules. Figure 1 shows the resulting amplifier module.

The amplifier chip was described in "MMIC HEMT Power Amplifier for 140 to 170 GHz" (NPO-30127), *NASA Tech Briefs*, Vol. 27, No. 11, (November 2003), page 49. To recapitulate: This is a three-stage MMIC power amplifier that utilizes HEMTs as gain elements. The amplifier was originally designed to operate in the frequency range of 140 to 170 GHz. The waveguide module is based on a previously developed lower frequency module, redesigned to support operation in the frequency range of 140 to 220 GHz.

Figure 2 presents results of one of several tests of the amplifier module — measurements of output power and gain as functions of input power at an output frequency of 150 GHz. Such an amplifier module has many applications to test equipment for power sources above 100 GHz.

Figure 1. The **Amplifier Is Packaged** in a WR5 waveguide module, with electric-field-plane alumina probes to interface the chip to the waveguide, and bypass capacitors to suppress low-frequency oscillations. The module is compact and can easily be integrated into a test system or with wafer probes.
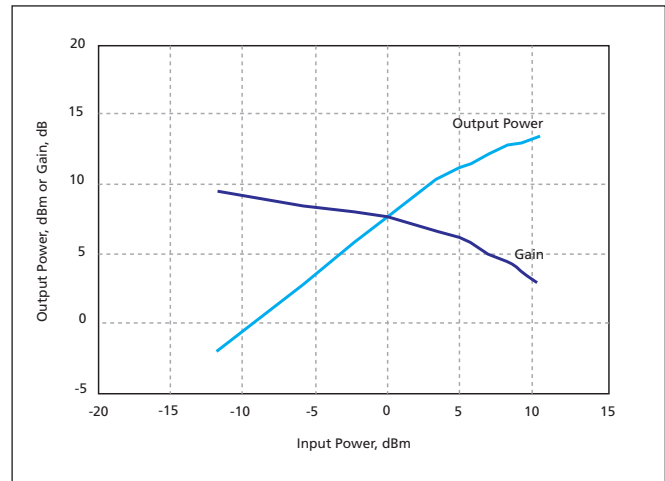
Aerial Videography From Locally Launched Rockets

Images of an event or scene are rapidly collected, processed, and displayed.

Stennis Space Center, Mississippi

A method of quickly collecting digital imagery of ground areas from video cameras carried aboard locally launched rockets has been developed. The method can be used, for example, to record rare or episodic events or to gather image data to guide decisions regarding treatment of agricultural fields or fighting wildfires.

The method involves acquisition and digitization of a video frame at a known time along with information on the position and orientation of the rocket and camera at that time. The position and orientation data are obtained by use of a Global Positioning System receiver and a digital magnetic compass carried aboard the rocket. These data are radioed to a ground station, where they are processed, by a real-time algorithm, into georeferenced position and orientation data. The algorithm also generates a file of transformation parameters that account for the variation of image magnification and distortion associated with the position and orientation of the camera relative to the ground scene depicted in the image. As the altitude, horizontal position, and ori-

entation of the rocket change between image frames, the algorithm calculates the corresponding new georeferenced position and orientation data and the associated transformation parameters.

The output imagery can be rendered in any of a variety of formats. The figure presents an example of one such format.

This work was done by Stacey D. Lyle of Conrad Blucher Institute for Surveying and Science at Texas A&M University—Corpus Christi for **Stennis Space Center**.

In accordance with Public Law 96-517, the contractor has elected to retain title to this invention. Inquiries concerning rights for its commercial use should be addressed to:
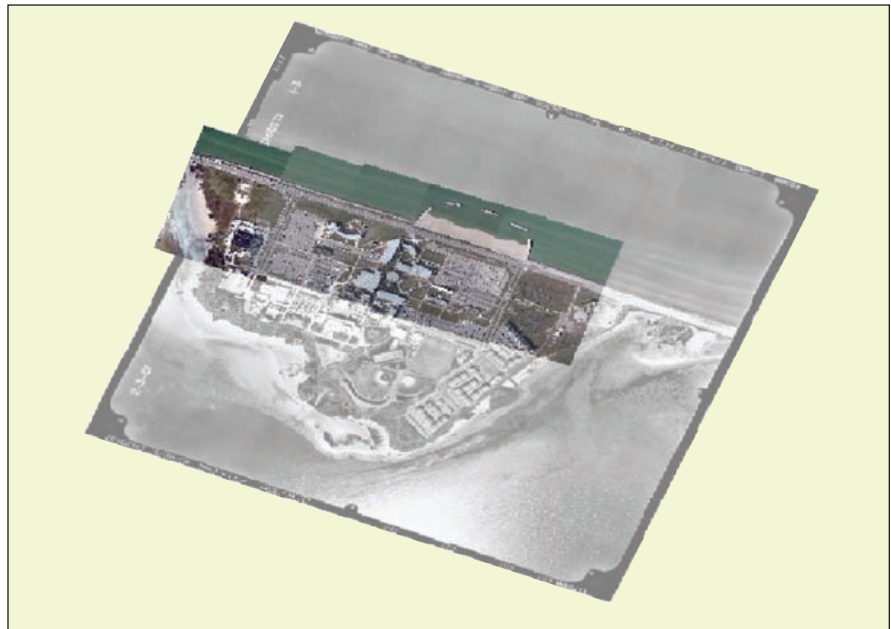
Texas A&M — Corpus Christi
6300 Ocean Dr.
Corpus Christi, Texas 78412
Phone No.: (361) 825-3712
E-mail: slyle@falcon.tamucc.edu
Refer to SSC-00214-1, volume and number of this NASA Tech Briefs *issue, and the page number.*

A **Digitized, Transformed Image** acquired from a video camera aboard a rocket was superimposed on a scan of an aerial image of a larger area that contains most of the video-image scene.

SiC Multi-Chip Power Modules as Power-System Building Blocks

Fault-tolerant power-supply systems could be constructed and expanded relatively inexpensively.

John H. Glenn Research Center, Cleveland, Ohio

The term "SiC MCPMs" (wherein "MCPM" signifies "multi-chip power module") denotes electronic power-supply modules containing multiple silicon carbide power devices and silicon-on-insulator (SOI) control integrated-circuit chips. SiC MCPMs are being developed as building blocks of advanced expandable, reconfigurable, fault-tolerant power-supply systems. Exploiting the ability of SiC semiconductor devices to operate at temperatures, breakdown voltages, and current densities significantly greater than those of conventional Si devices, the designs of SiC MCPMs and of systems comprising multiple SiC MCPMs are expected to afford a greater degree of miniaturization through stacking of modules with reduced requirements for heat sinking. Moreover, the higher-temperature capabilities of SiC MCPMs could enable operation in environments hotter than Si-based power systems can withstand.

The stacked SiC MCPMs in a given system can be electrically connected in series, parallel, or a series/parallel combination to increase the overall power-handling capability of the system. In addition to power connections, the modules have communication connections. The SOI controllers in the modules communicate with each other as nodes of a decentralized control network, in which no single controller exerts overall command of the system. Control functions effected via the network include synchronization of switching of power devices and rapid reconfiguration of power connections to enable the power system to continue to supply power to a load in the event of failure of one of the modules.

In addition to serving as building blocks of reliable power-supply systems, SiC MCPMs could be augmented with external control circuitry to make them perform additional power-handling functions as needed for specific applications: typical functions could include regulating voltages, storing energy, and driving motors. Because identical SiC MCPM building blocks could be utilized in a variety of ways, the cost and difficulty of designing new, highly reliable power systems would be reduced considerably.

Several prototype DC-to-DC power-converter modules containing SiC power-switching devices were designed and built to demonstrate the feasibility of the SiC MCPM concept. In anticipation of a future need for operation at high temperature, the circuitry in the modules includes high-temperature inductors and capacitors. These modules were designed to be stacked to construct a system of four modules electrically connected in series and/or parallel.

The packaging of the modules is designed to satisfy requirements for series and parallel interconnection among modules, high power density, high thermal efficiency, small size, and light weight. Each module includes four output power connectors — two for serial and two for parallel output power connections among the modules. Each module also includes two signal connectors, electrically isolated from the power connectors, that afford four zones for signal interconnections among the SOI controllers. Finally, each module includes two input power connectors, through which it receives power from an in-line power bus. This design feature is included in anticipation of a custom-designed power bus incorporating sockets compatible with "snap-on" type connectors to enable rapid replacement of failed modules.

The distributed control hardware and software enable power conversion to continue uninterrupted when as many as two

modules fail. Essential to distributed control is an arbitrated, shared communication bus. The arbitration protocol enables asynchronous bidirectional messaging without concern for data collisions and loss of messages. In tests of the four-module system in which failures of as many as two modules were simulated, measurement results showed that the system reconfigured itself rapidly enough in response to the failures to continue delivering power to a load without interruption and with minimum output-voltage sag. The transient time associated with a failure was found to be <5 ms, of which <350 μs was consumed by software and the rest was consumed by operation of bypass relays.

This work was done by Alexander Lostetter and Steven Franks of Arkansas Power Electronics International, Inc. for **Glenn Research Center**.

Inquiries concerning rights for the commercial use of this invention should be addressed to NASA Glenn Research Center, Innovative Partnerships Office, Attn: Steve Fedor, Mail Stop 4–8, 21000 Brookpark Road, Cleveland, Ohio 44135. Refer to LEW-18008-1.

Software

Automated Design of Restraint Layer of an Inflatable Vessel

A Mathcad computer program largely automates the design and analysis of the restraint layer (the primary load-bearing layer) of an inflatable vessel that consists of one or more sections having cylindrical, toroidal, and/or spherical shape(s). A restraint layer typically comprises webbing in the form of multiple straps. The design task includes choosing indexing locations along the straps, computing the load at every location in each strap, computing the resulting stretch at each location, and computing the amount of undersizing required of each strap so that, once the vessel is inflated and the straps thus stretched, the vessel can be expected to assume the desired shape.

Prior to the development of this program, the design task was performed by use of a difficult-to-use spreadsheet program that required manual addition of rows and columns depending on the numbers of strap rows and columns of a given design. In contrast, this program is completely parametric and includes logic that automatically adds or deletes rows and columns as needed. With minimal input from the user, this program automatically computes indexing locations, strap lengths, undersizing requirements, and all design data required to produce detailed drawings and assembly procedures. It also generates textual comments that help the user understand the calculations.

This program was written by Gary Spexarth of **Johnson Space Center**. *Further information is contained in a TSP (see page 1).*

This invention is owned by NASA, and a patent application has been filed. Inquiries concerning nonexclusive or exclusive license for its commercial development should be addressed to the Patent Counsel, Johnson Space Center, (281) 483-0837. Refer to MSC-23906.

TMS for Instantiating a Knowledge Base With Incomplete Data

A computer program that belongs to the class known among software experts as output truth-maintenance-systems (output TMSs) has been devised as one of a number of software tools for reducing the size of the knowledge base that must be searched during execution of artificial-intelligence software of the rule-based inference-engine type in a case in which data are missing. This program determines whether the consequences of activation of two or more rules can be combined without causing a logical inconsistency. For example, in a case involving hypothetical scenarios that could lead to turning a given device on or off, the program determines whether a scenario involving a given combination of rules could lead to turning the device both on and off at the same time, in which case that combination of rules would not be included in the scenario.

This program was written by Mark James of Caltech for **NASA's Jet Propulsion Laboratory**. *Further information is contained in a TSP (see page 1).*

This software is available for commercial licensing. Please contact Karina Edmonds of the California Institute of Technology at (626) 395-2322. Refer to NPO-42710.

Simulating Flights of Future Launch Vehicles and Spacecraft

Marshall Aerospace Vehicle Representation in C (MAVERIC) is a computer program for generic, low-to-high-fidelity simulation of the flight(s) of one or more launch vehicle(s) or spacecraft. MAVERIC is designed to accommodate multi-staged vehicles, powered serially or in parallel, with multiple engines, tanks, and cargo elements. Engines can be of jet or conventional rocket types, using either liquid or solid propellants.

MAVERIC includes generic subsystem software models for propulsion systems, mass properties, reaction control systems, aerodynamic properties, guidance systems, and navigation systems. Simulations can be started at points other than liftoff. Also included are guidance-system software models that accommodate the ascent, orbit, coasting, deorbiting, entry, terminal-area-energy-management, approach, and landing phases of flight.

Options to use different wind profiles and atmospheres are included. A Monte Carlo capability is provided for modeling dispersions associated with atmospheric effects (including winds), propulsion, navigation, aerodynamics, and mass properties. Failures of engines and other subsystems can be modeled. The program is written in the C programming language, which makes it possible for the program to have high degrees of modularity, reusability, and maintainability, thereby also facilitating modification for modeling new vehicles.

This program was written by James W. McCarter of **Marshall Space Flight Center**. *Further information is contained in a TSP (see page 1).*

This invention is owned by NASA, and a patent application has been filed. For further information, contact Sammy Nabors, MSFC Commercialization Assistance Lead, at sammy.a.nabors@nasa.gov. Refer to MFS-31989-1.

Control Code for Bearingless Switched-Reluctance Motor

A computer program has been devised for controlling a machine that is an integral combination of magnetic bearings and a switched-reluctance motor. The motor contains an eight-pole stator and a hybrid rotor, which has both (1) a circular lamination stack for levitation and (2) a six-pole lamination stack for rotation. The program computes drive and levitation currents for the stator windings with real-time feedback control. During normal operation, two of the four pairs of opposing stator poles (each pair at right angles to the other pair) levitate the rotor. The remaining two pairs of stator poles exert torque on the six-pole rotor lamination stack to produce rotation. This version is executable in a control-loop time of 40 μs on a Pentium (or equivalent) processor that operates at a clock speed of 400 MHz. The program can be expanded, by addition of logic blocks, to enable control of position along additional axes. The code enables adjustment of operational parameters (e.g., motor speed and stiffness, and damping parameters of magnetic bearings) through computer keyboard key presses.

This program was written by Carlos R. Morrison of **Glenn Research Center**. *Further information is contained in a TSP (see page 1).*

Machine Aided Indexing and the NASA Thesaurus

Machine Aided Indexing (MAI) is a Web-based application program for aiding the indexing of literature in the NASA Scientific and Technical Information (STI) Database. MAI was designed to be a convenient, fully interactive tool for determining the subject matter of documents and identifying keywords. The heart of MAI is a natural-language processor that accepts, as input, any user-supplied text, including abstracts, full documents, and Web pages. Within seconds, the text is analyzed and a ranked list of terms is generated. The 17,800 terms of the NASA Thesaurus serve as the foundation of the knowledge base used by MAI. The NASA Thesaurus defines a standard vocabulary, the use of which enables MAI to assist in ensuring that STI documents are uniformly and consistently accessible. Of particular interest to traditional users of the NASA Thesaurus, MAI incorporates a fully searchable thesaurus display module that affords word-search and hierarchy-navigation capabilities that make it much easier and less time-consuming to look up terms and browse, relative to lookup and browsing in older print and Portable Document Format (PDF) digital versions of the Thesaurus. In addition, because MAI is centrally hosted, the Thesaurus data are always current.

This program was written by Bill von Ofenheim for **Langley Research Center**. *For further information, access http://mai.larc.nasa.gov.*
LAR-17110-1

Arbitrating Control of Control and Display Units

The ARINC 739 Switch is a computer program that arbitrates control of two multi-function control and display units (MCDUs) between (1) a commercial flight-management computer (FMC) and (2) NASA software used in research on transport aircraft. (MCDUs are the primary interfaces between pilots and FMCs on many commercial aircraft.) This program was recently redesigned into a software library that can be embedded in research application programs. As part of the redesign, this software was combined with software for creating custom pages of information to be displayed on a CDU. This software commands independent switching of the left (pilot's) and right (copilot's) MCDUs. For example, a custom CDU page can control the left CDU while the FMC controls the right CDU. The software uses menu keys to switch control of the CDU between the FMC or a custom CDU page. The software provides an interface that enables custom CDU pages to insert keystrokes into the FMC's CDU input interface. This feature allows the custom CDU pages to manipulate the FMC as if it were a pilot.

This program was written by Michael M. Madden of **Langley Research Center** *and Paul C. Sugden of Unisys Corp. Further information is contained in a TSP (see page 1).*
LAR-17178-1

Web-Based Software for Managing Research

aeroCOMPASS is a software system, originally designed to aid in the management of wind tunnels at Langley Research Center, that could be adapted to provide similar aid to other enterprises in which research is performed in common laboratory facilities by users who may be geographically dispersed. Included in aeroCOMPASS is Web-interface software that provides a single, convenient portal to a set of project- and test-related software tools and other application programs. The heart of aeroCOMPASS is a user-oriented document-management software subsystem that enables geographically dispersed users to easily share and manage a variety of documents. A principle of "write once, read many" is implemented throughout aeroCOMPASS to eliminate the need for multiple entry of the same information. The Web framework of aeroCOMPASS provides links to client-side application programs that are fully integrated with databases and server-side application programs. Other subsystems of aeroCOMPASS include ones for reserving hardware, tracking of requests and feedback from users, generating interactive notes, administration of a customer-satisfaction questionnaire, managing execution of tests, managing archives of metadata about tests, planning tests, and providing online help and instruction for users.

This program was written by Sherwood T. Hoadley; Anthony M. Ingraldi; Kerry M. Gough; Charles Fox, Jr.; Catherine K. Cronin; Andrew G. Hagemann; Guy T. Kemmerly; and Wesley L. Goodman of **Langley Research Center**. *For further information, access http://aerocompass.larc.nasa.gov.*

This invention is owned by NASA, and a patent application has been filed. Inquiries concerning nonexclusive or exclusive license for its commercial development should be addressed to the Patent Counsel, Langley Research Center, at (757) 864-3521. Refer to LAR-16442.

Driver Code for Adaptive Optics

A special-purpose computer code for a deformable-mirror adaptive-optics control system transmits pixel-registered control from (1) a personal computer running software that generates the control data to (2) a circuit board with 128 digital-to-analog converters (DACs) that generate voltages to drive the deformable-mirror actuators. This program reads control-voltage codes from a text file, then sends them, via the computer's parallel port, to a circuit board with four AD5535 (or equivalent) chips. Whereas a similar prior computer program was capable of transmitting data to only one chip at a time, this program can send data to four chips simultaneously. This program is in the form of C-language code that can be compiled and linked into an adaptive-optics software system. The program as supplied includes source code for integration into the adaptive-optics software, documentation, and a component that provides a demonstration of loading DAC codes from a text file. On a standard Windows desktop computer, the software can update 128 channels in 10 ms. On Real-Time Linux with a digital I/O card, the software can update 1024 channels (8 boards in parallel) every 8 ms.

This program was written by Shanti Rao of Caltech for **NASA's Jet Propulsion Laboratory**. *Further information is contained in a TSP (see page 1).*

The software used in this innovation is available for commercial licensing. Please contact Karina Edmonds of the California Institute of Technology at (626) 395-2322. Refer to NPO-43107.

Ceramic Paste for Patching High-Temperature Insulation

Repairs can be performed by use of simple techniques.

Lyndon B. Johnson Space Center, Houston, Texas

A ceramic paste that can be applied relatively easily, either by itself or in combination with one or more layer(s) of high-temperature ceramic fabrics, such as silicon carbide or zirconia, has been invented as a means of patching cracks or holes in the reinforced carbon-carbon forward surfaces of a space shuttle in orbit before returning to Earth. The paste or the paste/fabric combination could also be used to repair rocket-motor combustion chambers, and could be used on Earth to patch similar high-temperature structures.

The specified chemical composition of the paste admits of a number of variations, and the exact proportions of its constituents are proprietary. In general, the paste consists of (1) silicon carbide, possibly with addition of (2) hafnium carbide, zirconium carbide, zirconium boride, silicon tetraboride, silicon hexaboride, or other metal carbides or oxides blended with (3) a silazane-based polymer.

Because the paste is viscous and sticky at normal terrestrial and outer-space ambient temperatures, high-temperature ceramic fabrics such as silicon carbide or zirconia fabric impregnated with the paste (or the paste alone) sticks to the damaged surface to which it is applied. Once the patch has been applied, it is smoothed to minimize edge steps as required [forward-facing edge steps must be ≤0.030 in. (≤0.76 mm) in the original intended space-shuttle application]. The patch is then heated to a curing temperature thereby converting it from a flexible material to a hard, tough material. The curing temperature is 375 to 450 °F (≈190 to 230 °C).

In torch tests and arc-jet tests, the cured paste was found to be capable of withstanding a temperature of 3,500 °F (≈1,900 °C) for 15 minutes. As such, the material appears to satisfy the requirement, in the original space-shuttle application, to withstand re-entry temperatures of ≈3,000 °F (≈1,600 °C).

This work was done by Steven J. Adam, James V. Tompkins, Gordon R. Toombs, Pete Hogensen, and Douglas G. Soden of The Boeing Co. for **Johnson Space Center**.

Title to this invention has been waived under the provisions of the National Aeronautics and Space Act {42 U.S.C. 2457(f)}, to The Boeing Company. Inquiries concerning licenses for its commercial development should be addressed to:

The Boeing Company
PO Box 2515
2201 Seal Beach Blvd.
Seal Beach, CA 90740-1515
Refer to MSC-23942, volume and number of this NASA Tech Briefs *issue, and the page number.*

Fabrication of Polyimide-Matrix/Carbon and Boron-Fiber Tape

Production costs can be reduced and compression strengths increased.

Langley Research Center, Hampton, Virginia

The term "HYCARB" denotes a hybrid composite of polyimide matrices reinforced with carbon and boron fibers. HYCARB and an improved process for fabricating dry HYCARB tapes have been invented in a continuing effort to develop lightweight, strong composite materials for aerospace vehicles. Like other composite tapes in this line of development, HYCARB tapes are intended to be used to build up laminated structures having possibly complex shapes by means of automated tow placement (ATP) — a process in which a computer-controlled multiaxis machine lays down prepreg tape or tows. The special significance of the present process for making dry HYCARB for ATP is that it contributes to the reduction of the overall cost of manufacturing boron-reinforced composite-material structures while making it possible to realize increased compression strengths.

The present process for making HYCARB tapes incorporates a "wet to dry" process developed previously at Langley Research Center. In the "wet to dry"

process, a flattened bundle of carbon fiber tows, pulled along a continuous production line between pairs of rollers, is impregnated with a solution of a poly(amide acid)

This **Photomicrograph** shows a cross of a specimen containing one layer of boron fibers.

in N-methyl-2-pyrrolidinone (NMP), then most of the NMP is removed by evaporation in hot air. In the present case, the polyamide acid is, more specifically, that of LaRC™ IAX (or equivalent) thermoplastic polyimide, and the fibers are, more specifically, Manganite IM7 (or equivalent) poly-acrylonitrile-based carbon filaments that have a diameter of 5.2 µm and are supplied in 12,000-filament tows.

The present process stands in contrast to a prior process in which HYCARB tape was made by pressing boron fibers into the face of a wet carbon-fiber/poly(amide acid) prepreg tape — that is, a prepreg tape from which the NMP solvent had not been removed. In the present process, one or more layer(s) of side-by-side boron fibers are pressed between dry prepreg tapes that have been prepared by the aforementioned "wet to dry" process. The multilayer tape is then heated to imidize the matrix material and remove most of the remaining solvent, and is pressed to consolidate the multiple layers into a dense tape.

For tests, specimens of HYCARB tapes and laminated composite panels made from HYCARB tape were prepared as follows: HYCARB tapes were fabricated as described above. Each panel was made by laying down ten layers of tape, containing, variously, one, two, or three boron-fiber plies and the remainder carbon-fiber-only plies (see figure). Each panel was made by laying down ten layers of tape. Each panel was then cured by heating to a temperature of 225 °C for 15 minutes, then pressing at 200 psi (≈1.4 MPa) while heating to 371 °C, holding at 371 °C for 1 hour, then continuing to hold pressure during cooling. Control specimens that were otherwise identical except that they did not contain boron fibers also were prepared. In room-temperature flexural tests, the HY-CARB specimens performed comparably to the control specimens; in room-temperature, open-hole compression tests, the HYCARB specimens performed slightly better, by amounts that increased with boron content.

This work was done by Harry L. Belvin and Roberto J. Cano of **Langley Research Center** *and Monte Treasure and Thomas W. Shahood of Textron Specialty Materials. Further information is contained in a TSP (see page 1).*

This invention is owned by NASA, and a patent application has been filed. Inquiries concerning nonexclusive or exclusive license for its commercial development should be addressed to the Patent Counsel, Langley Research Center, at (757) 864-3521. Refer to LAR-15852.

Protective Skins for Aerogel Monoliths

Viscous polymer precursors are applied, then polymerized before they can percolate in.

John H. Glenn Research Center, Cleveland, Ohio

A method of imparting relatively hard protective outer skins to aerogel monoliths has been developed. Even more than aerogel beads, aerogel monoliths are attractive as thermal-insulation materials, but the commercial utilization of aerogel monoliths in thermal-insulation panels has been inhibited by their fragility and the consequent difficulty of handling them. Therefore, there is a need to afford sufficient protection to aerogel monoliths to facilitate handling, without compromising the attractive bulk properties (low density, high porosity, low thermal conductivity, high surface area, and low permittivity) of aerogel materials. The present method was devised to satisfy this need.

The essence of the present method is to coat an aerogel monolith with an outer polymeric skin, by painting or spraying. Apparently, the reason spraying and painting were not attempted until now is that it is well known in the aerogel industry that aerogels collapse in contact with liquids. In the present method, one prevents such collapse through the proper choice of coating liquid and process conditions: In particular, one uses a viscous polymer precursor liquid and (a) carefully controls the amount of liquid applied and/or (b) causes the liquid to become cured to the desired hard polymeric layer rapidly enough that there is not sufficient time for the liquid to percolate into the aerogel bulk.

The method has been demonstrated by use of isocyanates, which, upon exposure to atmospheric moisture, become cured to polyurethane/polyurea-type coats. The method has also been demonstrated by use of commercial epoxy resins. The method could also be implemented by use of a variety of other resins, including polyimide precursors (for forming high-temperature-resistant protective skins) or perfluorinated monomers (for forming coats that impart hydrophobicity and some increase in strength).

This work was done by Nicholas Leventis, James C. Johnston, Maria A. Kuczmarski, and Mary Ann B. Meador of **Glenn Research Center**. *Further information is contained in a TSP (see page 1).*

Inquiries concerning rights for the commercial use of this invention should be addressed to NASA Glenn Research Center, Commercial Technology Office, Attn: Steve Fedor, Mail Stop 4–8, 21000 Brookpark Road, Cleveland, Ohio 44135. Refer to LEW-17605-1.

Code Assesses Risks Posed by Meteoroids and Orbital Debris

Lyndon B. Johnson Space Center, Houston, Texas

BUMPER II version 1.92e is a computer code for assessing the risk of damage from impacts of micrometeoroids and orbital debris on the International Space Station (ISS), including those parts of the ISS covered by shielding that affords partial protection against such impacts. (Other versions of BUMPER II have been written for other spacecraft.) Bumper II quantifies the probability of penetration of shielding and the damage to spacecraft equipment as functions of the size, shape, and orientation of the spacecraft; the parameters of its orbit;

failure criteria that quantify impact damage at the threshold of failure for each spacecraft surface; and the impact-damage resistance of each spacecraft surface as defined by "ballistic limit equations" that return the size of a failure-causing particle as a function of target parameters (including materials, configurations, thicknesses, and gap distances) and impact conditions (impact velocity and the density and shape of the impactor). BUMPER II version 1.92e contains several dozen ballistic limit equations that are based on results from

thousands of hypervelocity impact tests conducted by NASA on ISS shielding and other hardware, and on results from numerical simulations of impacts.

This program was written by Eric L. Christiansen and Justin Kerr of **Johnson Space Center***; Dana Lear, Jim Hyde, and Tom Prior of Lockheed Martin Corp.; and Russell Graves of The Boeing Company, Inc. For further information, contact the Johnson Commercial Technology Office at (281) 483-3809.*
MSC-23774

Asymmetric Bulkheads for Cylindrical Pressure Vessels
These bulkheads would offer advantages over prior concave, convex, and flat bulkheads.

Marshall Space Flight Center, Alabama

Asymmetric bulkheads are proposed for the ends of vertically oriented cylindrical pressure vessels. These bulkheads, which would feature both convex and concave contours, would offer advantages over purely convex, purely concave, and flat bulkheads (see figure). Intended originally to be applied to large tanks that hold propellant liquids for launching spacecraft, the asymmetric-bulkhead concept may also be attractive for terrestrial
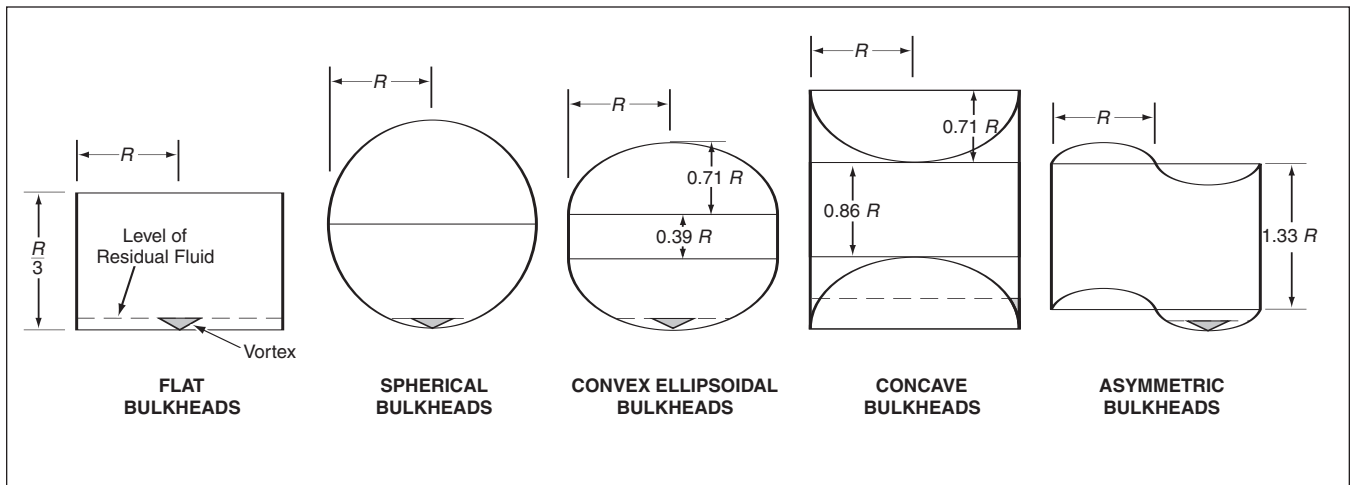
pressure vessels for which there are requirements to maximize volumetric and mass efficiencies.

A description of the relative advantages and disadvantages of prior symmetric bulkhead configurations is prerequisite to understanding the advantages of the proposed asymmetric configuration:
• In order to obtain adequate strength, flat bulkheads must be made thicker, relative to concave and convex bulk-

heads; the difference in thickness is such that, other things being equal, pressure vessels with flat bulkheads must be made heavier than ones with concave or convex bulkheads.
• Convex bulkhead designs increase overall tank lengths, thereby necessitating additional supporting structure for keeping tanks vertical.
• Concave bulkhead configurations increase tank lengths and detract from

These **Pressure-Vessel Configurations** have the same radius (*R*) and volume ($4\pi R^3/3$). The different shapes are shown here to illustrate the advantages and disadvantages of each. This is a representative but not exhaustive set of configurations, and is limited to single, non-nested pressure vessels for the sake of simplicity.

volumetric efficiency, even though they do not necessitate additional supporting structure.

- The shape of a bulkhead affects the proportion of residual fluid in a tank — that is, the portion of fluid that unavoidably remains in the tank during outflow and hence cannot be used. In this regard, a flat bulkhead is disadvantageous in two respects: (1) It lacks a single low point for optimum placement of an outlet and (2) a vortex that forms at the outlet during outflow prevents a relatively large amount of fluid from leaving the tank.
- A concave bulkhead also lacks a single low point for optimum placement of an outlet.

Like purely concave and purely convex bulkhead configurations, the proposed asymmetric bulkhead configurations would be more mass-efficient than is the flat bulkhead configuration. In comparison with both purely convex and purely concave configurations, the proposed asymmetric configurations would offer greater volumetric efficiency. Relative to a purely convex bulkhead configuration, the corresponding asymmetric configuration would result in a shorter tank, thus demanding less supporting structure. An asymmetric configuration provides a low point for optimum location of a drain, and the convex shape at the drain location minimizes the amount of residual fluid.

This work was done by Donald B. Ford of **Marshall Space Flight Center**.

This is the invention of a NASA employee, and a patent application has been filed. Inquiries concerning license for its commercial development may be addressed to the inventor:

Donald B. Ford
Phone No.: (256) 544-2454
E-mail: Donald.B.Ford@nasa.gov
Refer to MFS-31626-1.
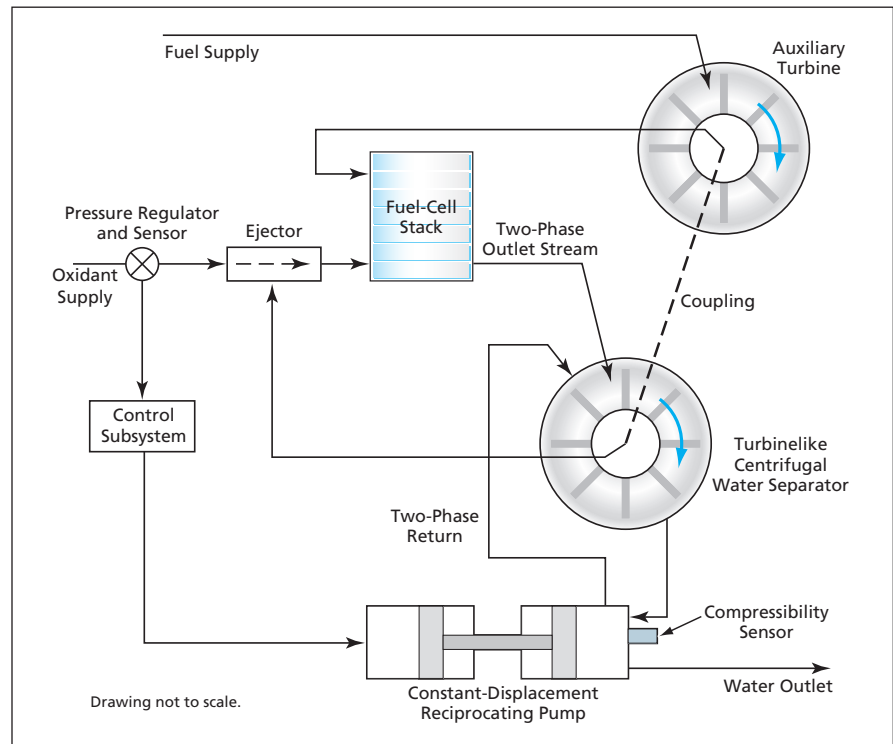
Self-Regulating Water-Separator System for Fuel Cells

This system would not depend on hydrophobic or hydrophilic surfaces.

Lyndon B. Johnson Space Center, Houston, Texas

A proposed system would perform multiple coordinated functions in regulating the pressure of the oxidant gas (usually, pure oxygen) flowing to a fuel-cell stack and in removing excess product water that is generated in the normal fuel-cell operation. The system could function in the presence or absence of gravitation, and in any orientation in a gravitational field.

Unlike some prior systems for removing product water, the proposed system would not depend on hydrophobicity or hydrophilicity of surfaces that are subject to fouling and, consequently, to gradual deterioration in performance. Also unlike some prior systems, the proposed system would not include actively controlled electric motors for pumping; instead, motive power for separation and pumping away of product water would be derived primarily from the oxidant flow and perhaps secondarily from the fuel flow. The net effect of these and other features would be to make the proposed system more reliable and safer, relative to the prior systems.

The proposed system (see figure) would include a pressure regulator and sensor in the oxidant supply just upstream from an ejector reactant pump. The pressure of the oxidant supply would depend on the consumption flow. In one of two control subsystems, the pressure of oxidant flowing from the supply to the ejector would be sensed and used to control the speed of a set of a reciprocating constant-displacement pump so that the volumetric flow of nominally incompressible water away from the system would slightly exceed the rate at which water was produced by the fuel cell(s).

The **Self-Regulating Water-Separator System** would derive its pumping and water-separating power from the flow of oxidant gas to the fuel-cell stack. Optionally, the fuel flow could be utilized as an auxiliary power source during operation of the fuel cell at low power.

The two-phase (gas/liquid water) outlet stream from the fuel cell(s) would enter the water separator, a turbinelike centrifugal separator machine driven primarily by the oxidant gas stream. A second control subsystem would utilize feedback derived from the compressibility of the outlet stream: As the separator was emptied of liquid water, the compressibility of the pumped stream would increase. The compressibility would be sensed, and an increase in compressibility beyond a preset point (signifying a decrease in water content below an optimum low level) would cause the outflow from the reciprocating pump to be diverted back to the separator to recycle some water.

This work was done by Arturo Vasquez, Kerri McCurdy, and Karla F. Bradley of **Johnson Space Center**.

This invention is owned by NASA, and a patent application has been filed. Inquiries concerning nonexclusive or exclusive license for its commercial development should be addressed to the Patent Counsel, Johnson Space Center, (281) 483-0837. Refer to MSC-23668.

Self-Advancing Step-Tap Drills

It is not necessary to apply axial drilling forces.

Lyndon B. Johnson Space Center, Houston, Texas

Self-advancing tool bits that are hybrids of drills and stepped taps make it possible to form threaded holes wider than about 1/2 in. (about 13 mm) without applying any more axial force than is necessary for forming narrower pilot holes. These self-advancing stepped-tap drills were invented for use by space-suited astronauts performing repairs on reinforced carbon/carbon space-shuttle leading edges during space walks, in which the ability to apply axial drilling forces is severely limited. Self-advancing stepped-tap drills could also be used on Earth for making wide holes without applying large axial forces.

A self-advancing stepped-tap drill (see figure) includes several sections having progressively larger diameters, typically in increments between 0.030 and 0.060 in. (between about 0.8 and about 1.5 mm). The tip section, which is the narrowest, is a pilot drill bit that typically has a diameter between 1/8 and 3/16 in. (between about 3.2 and about 4.8 mm). The length of the pilot-drill section is chosen, according to the thickness of the object to be drilled and tapped, so that the pilot hole is completed before engagement of the first tap section. Provided that the cutting-edge geometry of the drill bit is optimized for the material to be drilled, only a relatively small axial force [typically of the order of a few pounds (of the order of 10 newtons)] must be applied during drilling of the pilot hole. Once the first tap section engages the pilot hole, it is no longer necessary for the drill operator to apply axial force: the thread engagement between the tap and the workpiece provides the axial force to advance the tool bit.

Like the pilot-drill section, each tap section must be long enough to complete its hole before engagement of the next, slightly wider tap section. The precise values of t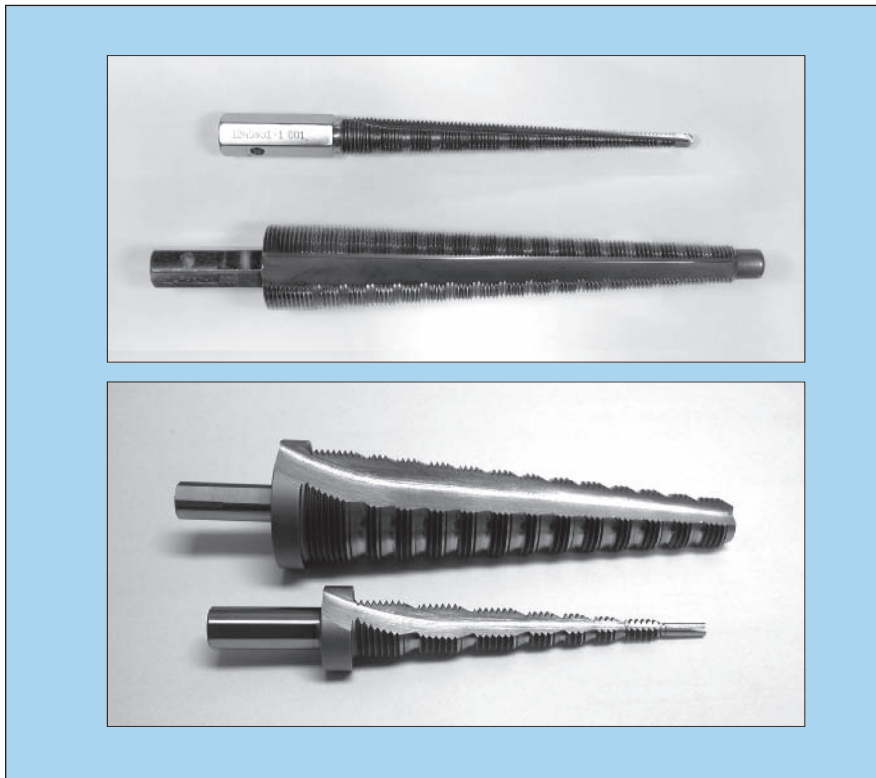he increments in diameter, the thread pitch, the rake angle of the tap cutting edge, and other geometric parameters of the tap sections must be chosen, in consideration of the workpiece material and thickness, to prevent stripping of threads during the drilling/tapping operation. A stop-lip or shoulder at the shank end of the widest tap section prevents further passage of the tool bit through the hole.

There is a large potential market for self-advancing stepped-tap drills in settings in which hand-held drills are used. Applied axial drilling forces can be quite large: it is not unusual to exert axial forces as much as 75 lb (≈330 N) when drilling holes up to about 1 in. (≈25 mm) in diameter. A person usually bears down on a drill with body weight to facilitate downward drilling, and drilling upward is extremely fatiguing. Repetitive drilling, which is often done in the construction industry, is fatiguing and limits worker productivity. Moreover, applying a large axial force with a hand-held drill can be dangerous: the drill bit can grab the workpiece, causing the workpiece to spin or tearing the drill from the worker's hand.

By making it unnecessary to apply large axial drilling forces, self-advancing stepped-tap drills could reduce fatigue while contributing to safety and productivity. Self-advancing stepped-tap drills could be made in a variety of designs optimized for making holes of specific diameters in specific workpiece materials having specific thicknesses. For applications in which the threads were not merely incidental to making the holes but were also needed to engage bolts, the tool bits would also be optimized for specific thread geometries.

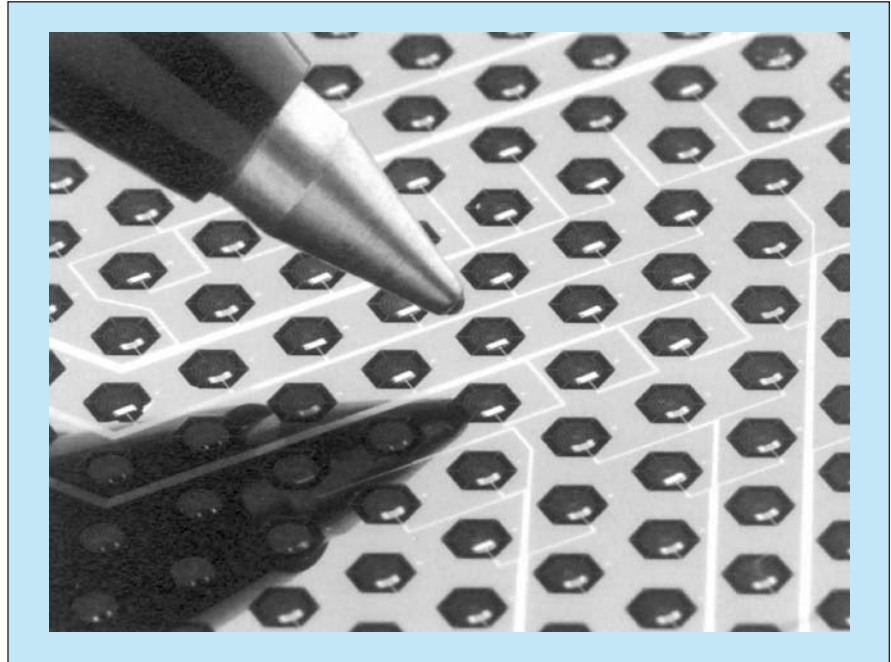These **Tool Bits** are examples of many variations on the basic theme of a self-advancing stepped-tap drill.

Array of Bolometers for Submillimeter-Wavelength Operation

This is a prototype of arrays for astrophysical imaging and photometry.

NASA's Jet Propulsion Laboratory, Pasadena, California

A feed-horn-coupled monolithic array of micromesh bolometers is undergoing development for use in a photometric camera. The array is designed for conducting astrophysical observations in a wavelength band centered at 350 µm. The bolometers are improved versions of previously developed bolometers comprising metalized Si_3N_4 micromesh radiation absorbers coupled with neutron-transmutation-doped Ge thermistors. Incident radiation heats the absorbers above a base temperature, changing the electrical resistance of each thermistor. In the present array of improved bolometers (see figure), the thermistors are attached to the micromesh absorbers by indium bump bonds and are addressed by use of lithographed, vapor-deposited electrical leads. This architecture reduces the heat capacity and minimizes the thermal conductivity to 1/20 and 1/300, respectively, of earlier versions of these detectors, with consequent improvement in sensitivity and speed of response.

The micromesh bolometers, intended to operate under an optical background set by thermal emission from an ambient-temperature space-borne telescope, are designed such that the random arrival of photons ("photon noise") dominates the noise sources arising from the detector and readout electronics. The micromesh is designed to be a highly thermally and optically efficient absorber with a limiting response time of about 100 µs. The absorber and thermistor heat capacity are minimized in order to give rapid speed of response. Due to the minimization of the absorber volume, the dominant source of heat capacity arises from the thermistor.

The array demonstrates a dark noise-equivalent power of $2.9 \cdot 10^{-17}$ W/$(Hz)^{1/2}$ and a mean heat capacity of 1.3 pJ/K at a detector temperature of 0.390 K from a 0.300 K cold plate. The optical efficiency of the bolometer and feedhorn array, measured by comparing the responses to blackbody calibration sources, lies between 0.4 and 0.6. Photon noise dominates over detector noise arising from phonon, Johnson, and amplifier noise, as measured under the design background conditions. The ratio of total noise to photon noise is found to be 1.21 at an absorbed optical power of 2.4 pW. The array shows high stability with excess noise found to be negligible at frequencies as low as 30 mHz.

This work was done by James Bock and Anthony Turner of Caltech for **NASA's Jet Propulsion Laboratory**. *Further information is contained in a TSP (see page 1).* NPO-30290

This **Array of Micromesh Bolometers** was designed for photometry at a wavelength of 350 µm. Each device includes a 725-µm-diameter micromesh absorber with a grid spacing of 72.5 µm and a grid filling factor of 0.077. A thermistor is located on one side of each absorber and is electrically addressed by two leads deposited on a single 18-µm-wide supporting member. The pixel spacing is 1.75 mm.

Delta-Doped CCDs as Detector Arrays in Mass Spectrometers

Improved performance is obtained with reduced size, mass, and power.

NASA's Jet Propulsion Laboratory, Pasadena, California

In a conventional mass spectrometer, charged particles (ions) are dispersed through a magnetic sector onto an MCP at an output (focal) plane. In the MCP, the impinging charged particles excite electron cascades that afford signal gain. Electrons leaving the MCP can be read out by any of a variety of means; most commonly, they are post-accelerated onto a solid-state detector array, wherein the electron pulses are converted to photons, which, in turn, are converted to measurable electric-current pulses by photodetectors. Each step in the conversion from the impinging charged particles to the output

current pulses reduces spatial resolution and increases noise, thereby reducing the overall sensitivity and performance of the mass spectrometer. Hence, it would be preferable to make a direct measurement of the spatial distribution of charged particles impinging on the focal plane.

The utility of delta-doped CCDs as detectors of charged particles was reported in two articles in *NASA Tech Briefs*, Vol. 22, No. 7 (July 1998): "Delta-Doped CCDs as Low-Energy-Particle Detectors" (NPO-20178) on page 48 and "Delta-Doped CCDs for Measuring Energies of Positive Ions" (NPO-20253) on page 50. In the present developmental miniature mass spectrometers, the above mentioned miniaturization and performance advantages contributed by the use of delta-doped CCDs are combined with the advantages afforded by the Mattauch-Herzog design. The Mattauch-Herzog design is a double-focusing spectrometer design involving an electric and a magnetic sector, where the ions of different masses are spatially separated along the focal plane of magnetic sector. A delta-doped CCD at the focal plane measures the signals of all the charged-particle species simultaneously at high sensitivity and high resolution, thereby nearly instantaneously providing a complete, high-quality mass spectrum. The simultaneous nature of the measurement of ions stands in contrast to that of a scanning mass spectrometer, in which abundances of different masses are measured at successive times.

Arrays of Bundles of Carbon Nanotubes as Field Emitters
Area-averaged current densities exceed those of arrays of single nanotubes.

NASA's Jet Propulsion Laboratory, Pasadena, California

Experiments have shown that with suitable choices of critical dimensions, planar arrays of bundles of carbon nanotubes (see figure) can serve as high-current-density field emitter (cold-cathode) electron sources. Whereas some hot-cathode electron sources must be operated at supply potentials of thousands of volts, these cold-cathode sources generate comparable current densities when operated at tens of volts. Consequently, array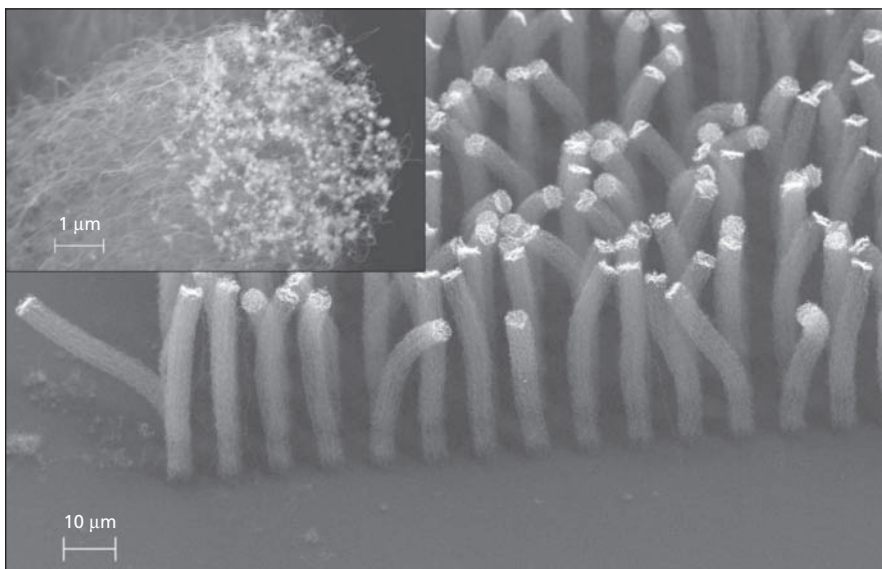s of bundles of carbon nanotubes might prove useful as cold-cathode sources in miniature, lightweight electron-beam devices (e.g., nanoklystrons) soon to be developed.

Prior to the experiments, all reported efforts to develop carbon-nanotube-based field-emission sources had yielded low current densities — from a few hundred microamperes to a few hundred milliamperes per square centimeter. An electrostatic screening effect, in which taller nanotubes screen the shorter ones from participating in field emission, was conjectured to be what restricts the emission of electrons to such low levels. It was further conjectured that the screening effect could be reduced and thus emission levels increased by increasing the spacing between nanotubes to at least by a factor of one to two times the height of the nanotubes. While this change might increase the emission from individual nanotubes, it would decrease the number of nanotubes per unit area and thereby reduce the total possible emission current. Therefore, to maximize the area-averaged current density, it would be necessary to find an optimum combination of nanotube spacing and nanotube height.

The present concept of using an array of bundles of nanotubes arises partly from the concept of optimizing the spacing and height of field emitters. It also arises partly from the idea that single nanotubes may have short lifetimes as field emitters, whereas bundles of nanotubes could afford redundancy so that the loss of a single nanotube would not significantly reduce the overall field emission.

In preparation for the experiments, planar arrays of bundles of carbon nanotubes having various bundle diameters, bundle heights, and bundle spacings were fabricated. The fabrication process can be summarized as follows: Electron-beam lithography was used to form planar arrays of iron dots having various thicknesses

This **Scanning Electron Micrograph** shows bundles of carbon nanotubes, each 70 μm high and 5 μm in diameter. The gaps between adjacent bundles are about 5 μm wide. The bundles stand up because their constituent nanotubes support each other. The inset is a magnified image of the top of one bundle, showing individual nanotube tips.

and having diameters and inter-dot spacings corresponding to the desired diameters and spacings of the carbon-nanotube bundles. The dots served as catalysts for the growth of carbon nanotubes: Bundles of multiwalled 20-nm-diameter carbon nanotubes were grown on the iron dots by chemical vapor deposition. The average height of the bundles was $70 \pm 2\mu m$. The heights of the bundles were found to depend on the thicknesses of the iron dots. The tallest bundles (112 μm high) were found on iron dots 8 μm thick.

In the experiments, field emission from these arrays was measured in a vacuum chamber by use of a 100-μm-diameter probe anode. The highest nondestructive area-averaged current densities (about 1.5 to 1.8 A/cm^2) were observed on arrays of bundles of 1- to 2-μm diameter and spacings of 5 μm at an applied electric field of about 4.5 V/μm.

This work was done by Harish Manohara and Michael Bronkowski of Caltech for **NASA's Jet Propulsion Laboratory**. *For further information, access the Technical Support Package (TSP)* **free on-line at www.techbriefs.com/tsp** *under the Physical Sciences category.*

Books & Reports

Staggering Inflation To Stabilize Attitude of a Solar Sail

A document presents computational-simulation studies of a concept for stabilizing the attitude of a spacecraft during deployment of such structures as a solar sail or other structures supported by inflatable booms. Specifically, the solar sail considered in this paper is a square sail with inflatable booms and attitude control vanes at the corners. The sail inflates from its stowed configuration into a square sail with four segments and four vanes at the tips. Basically, the concept is one of controlling the rates of inflation of the booms to utilize in mass-distribution properties to effect changes in the system's angular momentum.

More specifically, what was studied were the effects of staggering inflation of each boom by holding it at constant length for specified intervals between intervals of increasing length until full length is reached. The studies included sensitivity analyses of effects of variations in mass properties, boom lengths, rates of increase in boom length, initial rates of rotation of the spacecraft, and several asymmetries that could arise during deployment.

The studies led to the conclusion that the final attitude of the spacecraft could be modified by varying the parameters of staggered inflation. Computational studies also showed that by feeding back attitude and attitude-rate measurements so that corrective action is taken during the deployment, the final attitude can be maintained very closely to the initial attitude, thus mitigating the attitude changes incurred during deployment and caused by modeling errors. Moreover, it was found that by optimizing the ratio between the holding and length-increasing intervals in deployment of a boom, one could cause deployment to track a desired deployment profile to place the entire spacecraft in a desired attitude at the end of deployment.

This work was done by Marco Quadrelli and John West of Caltech for **NASA's Jet Propulsion Laboratory**. *Further information is contained in a TSP (see page 1).*
NPO-42176

Bare Conductive Tether for Decelerating a Spacecraft

A document describes a prototype of electrically conductive tethers to be used primarily to decelerate spacecraft and/or generate electric power for the spacecraft. Like prior such tethers, this tether is designed so that when it is deployed from a spacecraft in orbit, its motion across the terrestrial magnetic field induces an electric current. The Lorentz force on the current decelerates the spacecraft. Optionally, the current can be exploited to convert some orbital kinetic energy to electric energy for spacecraft systems. Whereas the conductive portions of prior such tethers are covered with electrical insulation except for end electrodes that make contact with the ionosphere, this tether includes a conductive portion that is insulated along part of its length but deliberately left bare along a substantial remaining portion of its length to make contact with the ionosphere. The conductive portions of the tether are made of coated thin aluminum wires wrapped around strong, lightweight aromatic polyamide braids. The main advantages of the present partly-bare-tether design over the prior all-insulated-tether design include greater resistance to degradation by the impact of monatomic oxygen at orbital altitude and speed and greater efficiency in collecting electrons from the ionosphere.

This work was done by Les Johnson, Jason Vaughn, Ken Welzyn, and Judy Ballance of **Marshall Space Flight Center***; Joe Carroll of Tether Applications; Enrico Lorenzini and Bob Estes of the Smithsonian Astrophysical Observatory; Pete Schuler, Hamid "Bob" Mojazza, and John Lennhoff of Triton Systems; and Kai Shen Hwang of Computer Sciences Corp. Further information is contained in a TSP (see page 1).*

This invention is owned by NASA, and a patent application has been filed. For further information, contact Sammy Nabors, MSFC Commercialization Assistance Lead, at sammy.a.nabors@nasa.gov. Refer to MFS-31490-1.

National Aeronautics and
Space Administration